AD-A149 520 DENSIFICATION OF SUBMICRON YSZ (YTTRIA-STBBILIZED ZIRCONIA) POWDERS WITH..(U) ILLINOIS UNIV AT URBANA DEPT OF CERAMIC ENGINEERING R C BUCHANAN ET AL. 1/1

UNCLASSIFIED 10 DEC 84 N00014-80-K-0969 F/G 11/2 NL

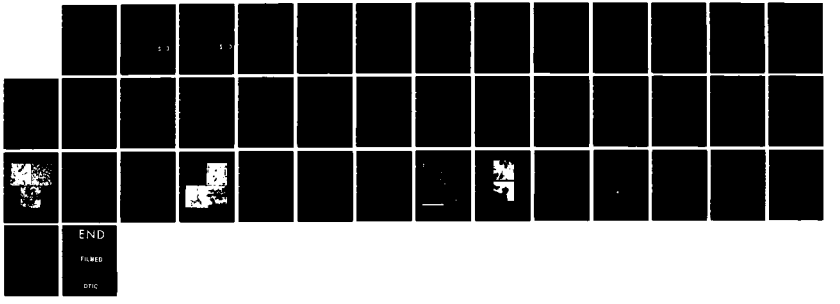

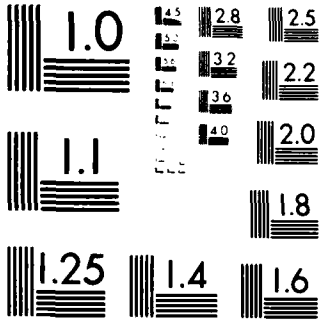

(12)

Final Report
Technical Report No. 9
Contract No.: US NAVY-N-00014-80-K-0969

Densification of Submicron YSZ Powders with Alumina and Borate Additives

DEPARTMENT OF CERAMIC ENGINEERING
UNIVERSITY OF ILLINOIS
URBANA, ILLINOIS

Final Report
Technical Report No. 9
Contract No.: US NAVY-N-00014-80-K-0969

Densification of Submicron YSZ Powders with Alumina and Borate Additives

by

R. C. Buchanan and D. M. Wilson

December 1984

Department of Ceramic Engineering
University of Illinois at Urbana-Champaign
105 S. Goodwin Avenue
Urbana, IL 61801

Research was supported by the Office of Naval Research
Department of the Navy
Contract No. US NAVY-N-00014-80-K-0969

SECURITY CLASSIFICATION OF THIS PAGE

REPORT DOCUMENTATION PAGE

1a. REPORT SECURITY CLASSIFICATION
Unclassified

1b. RESTRICTIVE MARKINGS

2a. SECURITY CLASSIFICATION AUTHORITY

3. DISTRIBUTION/AVAILABILITY OF REPORT
W... DISTRIBUTION STATEMENT A
Approved for public release
Distribution Unlimited
...opies to
...ividuals and
...NR Program.

2b. DECLASSIFICATION/DOWNGRADING SCHEDULE

4. PERFORMING ORGANIZATION REPORT NUMBER(S)
Report No. 9

5. M... ...ER(S)
Office of Naval Research US NAVY-N-00014-80-K-0969

6a. NAME OF PERFORMING ORGANIZATION
University of Illinois

6b. OFFICE SYMBOL *(If applicable)*

7a. NAME OF MONITORING ORGANIZATION

6c. ADDRESS *(City, State and ZIP Code)*
Department of Ceramic Engineering
105 S. Goodwin Avenue
Urbana IL 61801

7b. ADDRESS *(City, State and ZIP Code)*

8a. NAME OF FUNDING/SPONSORING ORGANIZATION
Office of Naval Research

8b. OFFICE SYMBOL *(If applicable)*

9. PROCUREMENT INSTRUMENT IDENTIFICATION NUMBER

8c. ADDRESS *(City, State and ZIP Code)*
Division of Materials Research
Arlington, VA 22217

10. SOURCE OF FUNDING NOS.

PROGRAM ELEMENT NO.	PROJECT NO.	TASK NO.	WORK UNIT NO.

11. TITLE *(Include Security Classification)*
Densification of Submicron YSZ Powders with Alumina and Borate Additives

12. PERSONAL AUTHOR(S)
R. C. Buchanan and D. M. Wilson

13a. TYPE OF REPORT	13b. TIME COVERED	14. DATE OF REPORT (Yr., Mo., Day)	15. PAGE COUNT
Final	FROM 12/1/83 TO 11/30/84	12/10/84	

16. SUPPLEMENTARY NOTATION

17. COSATI CODES		
FIELD	GROUP	SUB. GR.

18. SUBJECT TERMS *(Continue on reverse if necessary and identify by block number)*
ZrO_2, YSZ, Al_2O_3 doping, Low temperature sintering.

19. ABSTRACT *(Continue on reverse if necessary and identify by block number)*

SEE NEXT PAGE

20. DISTRIBUTION/AVAILABILITY OF ABSTRACT
UNCLASSIFIED/UNLIMITED ☒ SAME AS RPT. ☐ DTIC USERS ☐

21. ABSTRACT SECURITY CLASSIFICATION
Unclassified

22a. NAME OF RESPONSIBLE INDIVIDUAL

22b. TELEPHONE NUMBER *(Include Area Code)*

22c. OFFICE SYMBOL

DD FORM 1473, 83 APR EDITION OF 1 JAN 73 IS OBSOLETE.

SECURITY CLASSIFICATION OF THIS PA...

ABSTRACT

SECURITY CLASSIFICATION OF THIS PAGE

Precipitated yttria (8.0 wt%) stabilized zirconia powders (YSZ) were sintered in the range 1150°-1350°C using Al_2O_3 and B_2O_3 as flux additions. A (2:1) Al_2O_3:B_2O_3 additive mixture at ~2 vol% concentration, gave significant densification when sintered at 1200°C/1 hr. Washing of the powders to remove residual Cl was necessary to achieve high densification belwo 1300°C. Samples obtained were optically translucent at 1 mm thickness with average grain size 0.2-0.4 μm. Mechanical, thermal and electrical properties were not degraded by the flux additions to YSZ. Densification by liquid phase sintering was determined for both B_2O_3 and Al_2O_3. Excess Al_2O_3 was found to exist as discrete particles in the YSZ matrix. Depletion of yttria from the grain matrix was observed with the flux additions but non-cubic phase transitions were not evident.

SECURITY CLASSIFICATION OF THIS PAGE

Densification of Submicron YSZ Powders With Alumina and Borate Additives

R. C. Buchanan and D. M. Wilson

INTRODUCTION

Yttria-stabilized zirconia(YSZ) has found extensive use in solid electrolyte and high strength applications due both to its high electrical conductivity and superior phase stability compared to the calcia-stabilized zirconia modification (CSZ). For these purposes, the fabrication of highly dense, uniform microstructures is essential. Optical applications such as transluscent lamp envelopes or IR sensor windows may also be possible with further refinement in processing and with decreased porosity.

Traditionally sintered in excess of 1700°c, zirconia has been densified at temperatures below 1400°C with the use of ultrafine powders and improved processing techniques.[1,2] In addition to energy saving considerations, low temperature densification has several advantages in zirconia systems. For example, reduced sintering temperatures may allow single step firing of electrode-YSZ composites. The reduced grain sizes produced have several inherent advantages, including reduced flaw and pore size and the retention of tetragonal grains (G.S. < 0.2 microns) with the consequent increase in fracture strength and toughness. Additionally, photon scattering in the IR and optical regions can be minimized by grain sizes which are smaller than the

incident wavelength, thereby reducing scattering and optical absorption.[3]

Sintering aids such as TiO_2, Fe_2O_3, SiO_2 and Al_2O_3 have been used to enhance densification in zirconia.[4,5] For instance, SiO_2 has been shown to be effective in reducing sintering temperatures in zirconia, but it has a detrimental effect on the electrical conductivity due to the formation of a glassy intergranular phase.[6,7] Additionally, the affinity of silica-rich boundary phases for stabilizing oxides in zirconia (especially Ca) is high, which can lead to destabilization in the matrix grains as the stabilizing oxide is drawn from the grain interior into the amorphous boundary regions.[8,9]

Al_2O_3 additives have been chosen for YSZ which is to be used for electrolyte applications, since alumina has little or no detrimental effect on bulk conductivity.[10,11,12] The Al_2O_3 additions aid densification in YSZ in amounts up to 1 mol% (0.08 wt%).[5,13] The mechanisms for densification enhancement have been the subject of much discussion. Radford et al.[5] (YSZ and CSZ), Mallinckrodt[8] (CSZ) and Takagi[14] (CSZ) have attributed enhanced sintering with Al_2O_3 additions to the presence of a low melting boundary phase formed by the dopant, the stabilizing oxide and existing impurities such as MgO, SiO_2 and CaO. Numerous eutectics can, in fact, be formed with these components below 1500°C. Alumina has been detected by selected area EDS analysis in three grain intersections in both CSZ and YSZ along with associated Ca, Mg and Si impurities.[10,14,15]

However, several studies using high resolution TEM microscopy on higher purity YSZ compositions have noted the absence of a continuous intergranular amorphous phase.[16,17,13] The alumina, which is only slightly soluble in YSZ ($\sim$ 0.1 mol% at 1300°C), was present primarily as discrete, crystalline inclusions often associated with amorphous SiO_2-rich "cusps". Nevertheless, densification, which primarily occurs by grain boundary transport in submicron

zirconia powders, was found to be accelerated by small amounts of the alumina-rich boundary liquid.

B_2O_3 has been investigated as a liquid phase sintering aid for zirconia by several authors. Hyatt et.al.[18] noted no increase in densification with B_2O_3 additions, but this may have resulted from volatilization of boron oxide at the high temperatures (1700°C) used. Sazanova et al.[19] likewise noted no enhanced sintering of YSZ with B_2O_3 additions. Additionally, boron oxide had no effect on the cubic phase content of a partially stabilized YSZ, indicating a lack of reactivity. Conversely, B_2O_3 was shown to effect a significant decrease in the sintering temperature of a submicron CSZ powder from 1500°C to 1200°C.[20] Enhanced densification was attributed to the formation of a low-melting calcium borate melt phase, ($2CaO \cdot B_2O_3$), as boron oxide was ineffective in densifying both the yttria-stabilized and unstabilized powders.[21]. In the case of YSZ, some destabilization (up to 7%) of the fully stabilized grains occured, though to a lesser extent than in CSZ, indicating the formation of a yttria-rich borate phase. However, liquid phase sintering would not be expected to occur by this mechanism, as no liquid is formed in the B_2O_3 Y_2O_3 system until 1373°C.

The system $Al_2O_3 \cdot B_2O_3$ has been fairly extensively studied. Two compounds exist in the system with Al_2O_3-B_2O_3 ratios of 9:2 and 2:1, respectively. The $9Al_2O_3 \cdot 2B_2O_3$ compound melts near 1900°C and is utilized for refractory furnace linings and catalyst supports.[3,23] The 2:1 compound melts incongruently at 1035°C giving the 9:2 compound and a liquid phase. The rate of formation of $9Al_2O_3 \cdot 2B_2O_3$ is somewhat slow at these temperatures and does not, therefore, result in volatilization of boron as HBO_3.

Kelin reported B_2O_3 to be an effective sintering aid up to a level of 1.0 wt% for a corundum ceramic containing 1.0 wt% of both CaO and SiO_2[24].

Sintering temperatures were reduced 80°C and mechanical strength was also increased. Further boron additions resulted in decreased strength and densification, possibly due to excessive liquid formation and volatilization of boron.

In this study, the Al_2O_3-B_2O_3 additive system was investigated as a sintering aid for ultrafine YSZ powders. It was anticipated that the high fluidity and potential compatibility of B_2O_3 with stabilized zirconia could be combined with the apparent reactivity of the alumina-rich melts with zirconia to produce an effective low-temperture liquid phase sintering aid. The objective was to minimize the total additive level in order to reduce the detrimental effect of intergranular phases on electrical conductivity and high temperature strength, while simultaneously producing a completely dense fired body.

EXPERIMENTAL

The powders used in this study were fully stabilized, precipitated 8.0 wt% (4.5 mol%) yttria stabilized zirconia.* A typical lot analysis for these powders is given in Table I. The Al_2O_3 additives were prepared from fine-grained reagant grade (>99%) aluminum hydroxide which was calcined for 2 hours at 600°C to form the oxide. An average particle size of 10-15 microns resulted but this was reduced considerably by subsequent milling. Reagant grade (>99%) anhydrous boron oxide was used as the B_2O_3 source.

Residual chlorine, shown by Scott et. al.[25] to inhibit low temperature densification in zirconia compacts, was removed by washing in distilled water. Dilute (1 vol%) suspensions were subjected to ultrasonic vibrations

* Zircar Corporation, Florida, New York

for 15 minutes, followed by centrifugation and the decanting of the supernate liquid. Four washings were sufficient to reduce the chlorine content of the powders to less than 0.04 wt%.

Batches of 50 g were prepared with Al_2O_3 and B_2O_3 additions of 0-3.24 wt% and 0-10 wt%, respectively. The batches were ball milled in a 60:40 solution of isopropanol and deionized water for 13 1/2 hours to reduce agglomeration. Polypropylene jars and zirconia balls were used to minimize contamination. An optimized binder/lubricant mixture of 1.0 wt% carbowax 4000, 1.0 wt% PVA, 0.25 wt% stearic acid and 0.06 wt% dibutyl phthalate was added for the final 1 1/2 hour of milling. The milled suspensions were spray dried** and pellets 1.6 cm in diameter and approximately 1.5 mm thick were pressed uniaxially at 221 Mpa (32,000 psi). Weight loss data indicated water contents near 3 wt%.

Firing was carried out on Pt foil in a $MoSi_2$ resistance furnace in the range 1050-1350°C. Samples fired for less than one half hour were initally heated to 1000°C in a Kanthal-would furnace, transferred to the $MoSi_2$ furnace at 1275°C for the designated sintering times and then returned to the Kanthal furnace for eventual cooling. Samples containing B_2O_3 were air-quenched from 800°C by removing them from the furnace to eliminate cracking due to a Y_2O_3-B_2O_3 phase transformation to be discussed later.

Sintered densities were determined by the water displacement technique. Using the lattice parameter data of Tuohig[26], the theoretical density of 8 wt% YSZ was determined to be 6.022 g/cm^3. Theoretical densities for samples containing lower density alumina and borate additives were calculated using a series mixing formula. Densities decreased progressively with increased additive contents, with the value for (YSZ + 0.65 wt% Al_2O_3 + 0.35 wt% B_2O_3)

** Buechi Laboratory Spray Dryer, Brinkman Instruments, New Jersey

being 5.96 g/cm^3.

A DuPont 1090 Thermal Analyzer System was used to obtain DTA and TGA data for raw material consitutents and for powder mixtures in the system Al_2O_3-B_2O_3-Y_2O_3-ZrO_2. The TGA data was supplemented by measurements of fired weight loss on both powders and pressed pellets in the range 1100-1350°C. Thermal expansion measurements were carried out on sample bars using the TMA attachment.

Microstructures were analyzed by SEM, TEM and EDS microanalysis techniques. Grain sizes were determined from SEM photomicrographs of polished and thermally etched sections, using the line intersection techniques of Mendelsohn[27]. TEM samples were prepared using a ball cratering device*** followed by < 10 hours ion milling, thereby assuring a minimum of milling artifacts. DC electrical resistivity was measured using a Hewlett-Packard 4260A Universal bridge. Specimens were polished plane parallel and provided with Pt paste electrodes, which were fired at 800°C in air. Measurements were made in air up to 900°C.

Infrared transmission spectra were obtained for polished, thinned samples using a Nicolet FT-IR spectrophotometer in the wavelenth range 1.6-16.6 microns.

RESULTS AND DISCUSSION

Figure 1 shows SEM photomicrographs of the as-received, milled and pressed YSZ powders. The powders as-received were highly agglomerated (Fig. 1a), with average agglomerate sizes being in the range 10-15 μm, which after 13.5 hr. ball milling was reduced to ~0.5 μm (Fig. 1b). A pressed section

*** VSZ Ball Cratering Instrument, The Technology Shop, Inc., Sudbury, Mass.

of the milled powder is shown in (Fig. 1c). The smaller sized agglomerates, while still residually present, were homogeneously distributed, a condition necessary for complete pore elimination during sintering.[9,10]

DTA heating and cooling curves are shown in Fig. 2 for (1:1) Y_2O_3:B_2O_3 and (2:1) Al_2O_3:B_2O_3 powder mixtures. The (1:1) Y_2O_3:B_2O_3 mixture showed, on heating, an apparant phase formation at 720°C and melt endotherms at 760° and 1120°C. On cooling, a sharp exotherm was obtained at 600°C which was attributed to the crystallization of a phase from a yttria-borate melt existing above 760°C. Little work has been done in establishing phase relationships in the Y_2O_3:B_2O_3 system, thus the DTA events could not be directly related to known phase changes. In any event, the phase change associated with the 600°C crystallization peak caused cracking in YSZ samples containing B_2O_3 when these were furnace cooled. The cracking was attributed to thermal expansion mismatch between the crystallized and YSZ matrix phases and could be eliminated by quenching of the sintered YSZ plus B_2O_3 samples from 800°C, resulting in the suppression of the 600°C crystallization peak as well. This cooling procedure was, therefore, adapted for all B_2O_3 containing samples.

Fig. 2 also shows the DTA trace for the (2:1) Al_2O_3:B_2O_3 powder mixture. Phase reactions occur between 900°C and 1200°C on heating, which can be attributed to the phase formation (~930-1000°C) and subsequent melting (~ 1035°C) of the 2:1 compound followed by crystallization of the 9:2 compound and coexistence with the liquid phase above 1035°C. This (2:1) Al_2O_3:B_2O_3 additive mixture to YSZ gave optimally dense samples at sintering temperatures of 1200-1275°C/1 hr.

Fig. 3 shows the densificatin behavior, at 1200°C/1 hr., of pressed YSZ pellets incorporating varying amounts of B_2O_3, Al_2O_3 and an optimal (0.065 wt%

Al_2O_3) mixture containing increasing amounts of B_2O_3 all added for the purpose of accelerating sintering of the YSZ. Density achieved by the base YSZ pellets at 1200°C/1 h was approximately 83% of theoretical (6.022 g/cm^3). This high degree of densification in undoped compacts can be attributed to the small PS, homogeneus and small agglomerate size distribution as well as to the liquid forming impurities in the starting powders.

Additions of B_2O_3 were found to inhibit densification in YSZ, confirming earlier observations by Sazanosva[19]. Only for B_2O_3 additions of ~10 wt% (~ 20 vol%) was significant densification (98.9 % ThD) achieved at 1200°C/1 h. In contrast, additions of Al_2O_3 to YSZ resulted in significant densification enhancement, the optimal additive level being approximately 0.65 wt% Al_2O_3. This is in agreement with the work of Radford et.al.[11] which showed a similar optimal Al_2O_3 additive level.

The densification enhancement with Al_2O_3 additions can be attributed to formation of low melting eutectics with existing impurities. Al_2O_3 additions beyond the optimal level indicated would, therefore: a) decrease the amount of melt formed, b) decrease the melt viscosity, c) increase the concentration of discrete particles in the YSZ matrix, and d) result in decreased densification rate, as observed. Thus, Al_2O_3 additions beyond the optimum would be expected to increase the liquid viscosity and also form discrete particles within the YSZ matrix, both conditions leading to a decrease in mass transport and in densification rates

Additions of B_2O_3 to the optimal YSZ-Al_2O_3 formulation, (YSZ + 0.65 wt% Al_2O_3) further accelerated the sintering rate. Complete densification for the washed (essentially Cl free) YSZ powder was achieved at 1200°C/1 h (Fig. 3). The use of unwashed powder significantly slowed densification, confirming the deleterious effect of Cl on the sintering kinetics. The optimal B_2O_3 addition

to the 0.65 wt% Al_2O_3 was found to be 0.35 wt%. This (2:1) Al_2O_3:B_2O_3 mixture, which melts incongruently at 1035°C, as indicated, would assure the presence of a highly fluid liquid at 1200°C resulting in the rapid densification rates observed. The observed decrease in density with higher B_2O_3 contents could result from an increase in the lower density vitreous phase as well as from possible crystallization of second phases, selective leaching of Y_2O_3 from the YSZ matrix and loss of boron.

Some insights into the sintering reactions described in Fig. 3 may be gained from examination of the reacted additive mixtures as presented Fig. 4. These figures show reactions for milled powder mixtures (not compacted) after heating to 1200°C/0.5-2 h in covered Pt. crucibles. Figs. 4a and 4b show, respectively, a near amorphous B_2O_3 compact and the essentially non-wetting conditions which existed at 1200°C/0.5 hr. when B_2O_3 was added to the YSZ in a 1:1 ratio. In contrast, Fig. 4c shows for the (2:1) Al_2O_3:B_2O_3 mixture, Al_2O_3 grains partially dissolved and enveloped by densely packed acicular crystals ~0.3 μm in diameter and 3-5 μm in length. The presence of these crystals, presumed to be of composition $9Al_2O_3$:$2B_2O_3$, illustrate the incongruent melting conditions previously referred to, and the existence of substantial liquid phase at the soak temperature (1200°C/0.5 hr.). Fig. 4d shows the reaction for a (2:1) YSZ:Al_2O_3 mixture at 1200°C/2 h. A clustering and apparent bonding of YSZ particles around the larger Al_2O_3 grains was observed, indicating some liquid phase formation, but small crystallite formation was less evident. The reactions of the different additive mixtures, therefore, are very much in keeping with the densification behaviour described in Fig. 3 for the doped YSZ.

Fig. 5 shows temperature dependence of the densification for YSZ, (YSZ + Al_2O_3 (0.325 wt%)) and (YSZ + Al_2O_3 (0.65 wt %) + B_2O_3 (0.35 wt%)) samples in

the range 1050-1350°C/0.5 h. All samples showed an increase in densification rate with temperature, the effect being much more pronounced for the additive YSZ samples. The (Al_2O_3 + B_2O_3) additive samples achieved maximum density at about 1200°C with a slight decrease as the soak temperature was increased due to possible loss of boron and simultaneous pore expansion. The strong increase in densificatin compared with the YSZ samples indicated the presence of relatively large amounts of a reactive intergranular liquid phase.

In the case of alumina additions, densification was also enhanced, but the similarities of the curves would indicate that Al_2O_3 was merely enhancing the effectiveness of the intergranular liquid formed by the existing impurities in the YSZ samples.

Fig. 6 shows the time dependence of densification at 1200°C for the YSZ and additive samples as in Fig. 5. The observed densification rates could be inferred from Figs. 3 and 5 except that Cl removal (washed sample) is seen to have had a pronounced effect on the sintering behavior of the (Al_2O_3 + B_2O_3) additive samples. With Al_2O_3 additions, the effect was less marked since essentially all of the residual Cl was eliminated by heating above 1275°C. Fig. 7 shows the short time shrinkage behavior for the YSZ and additive samples at 1275°C. Relative densities acheived after 20 min. wre in the range 65-99% for the differen samples. The two slopes identified for the YSZ and (YSZ + Al_2O_3 samples are indicative of initial particle rearrangment followed by a solution-precipitation densification mechanism in the presence of a liquid phase. These processes were less distinguishable for the B_2O_3 containing sample, which would indicate that substantially higher liquid phase was present at the sintering temperature and that rearrangement was the dominant sintering mechanism.

Table 2 gives density data for the samples studied as a function of soak

time and temperature. Densities generally increased with temperature and soak time except for those samples containing B_2O_3. Comparison of the YSZ and Al_2O_3 additive samples showed slightly lower ultimate densities for the latter, likely due to pore clusters which were often associated with undissolved Al_2O_3 particles. A lower concentration of such particles would, therefore, account for the higher densities achieved with the 0.325 wt% as compared to the 0.65 wt% Al_2O_3 samples under equivalent conditions.

For the combined Al_2O_3 + B_2O_3 samples the higher Al_2O_3 mixture seemed optimum, although rapid densification was achieved with the other mixtures as well. B_2O_3-containing samples all showed a decrease in density at the higher soak temperatures and times attributed in part to loss of boron. Table 3, which shows comparative weight loss data for the YSZ and additive samples, gives evidence of this weight loss with increasing B_2O_3 content. Background loss from the YSZ sample, which was washed and heat treated at 1100°C/1 h to eliminate moisture, carbonate and organic residues, was taken to be that of Cl and possibly sulfate residues. Estimated loss of B_2O_3 over the temperature span 1100-1350°C/4 h was in the range 11-19 wt% of the added B_2O_3, with most loss occurring at 1350°C.

The loss of boron from the samples resulted in a decrease in density, due to an increase in pore size as illustrated in Fig. 8. This figure shows SEM photomicrographs of polished and thermally etched sections of the (YSZ + 0.65 wt% Al_2O_3 + 0.35 wt% B_2O_3) samples after sintering at 1200°C/1.5 h (Fig. 8b) and 1350°C/4 h (Fig. 8d). Some clustering of pores was observed in both samples, but pore sizes (not concentration) were significantly enlarged at 1350°C. This reflected an accomodation to the higher vapor pressure of the B_2O_3 in the otherwise dense compact at 1350°C. Figs. 8a and 8c show, for comparison, the pore structure of the YSZ and (YSZ + 0.325 Al_2O_3) samples

sintered at 1275°C/4 h. Significantly less densification had taken place in the YSZ sample, as evidence by the larger distributed pore volume and smaller average grain size, in contrast to the Al_2O_3 additive sample which was dense and essentially pore free. Residual porosity was located exclusively at grain intersections.

Grain sizes determined on dense sintered samples under equivalent conditions were largest for (Al_2O_3 + B_2O_3) and smallest for the YSZ samples, in line with the observed sintering kinetics and dopant effectiveness. Average grain size ranges were 0.2-0.4 μm which may be contrasted to the 1-2 μm size of inclusions found in Al_2O_3 samples. EDS analysis of the inclusions showed them to be Al rich, indicating their origin to be undissolved Al_2O_3 particles.

Fig. 9a shows a TEM photomicrograph (magnification 230 Kx) of the (YSZ + 0.325 wt% Al_2O_3) sample. For both the YSZ and Al_2O_3 additive samples, liquid accumulation (greater for the Al_2O_3 doped) occurred mainly a 3 grain intersections, in contrast to B_2O_3 samples (Fig, 9b) where liquid was distributed also along the grain boundaries, a result of the higher liquid content at the sintering temperature. No second phases or inclusions were detected in the grain boundary regions, nor was there evidence of tetragonal (or monoclinic) phase formation in the YSZ grains. This was confirmed also by X-ray diffraction analysis on the sintered samples.

Data from EDS elemental analysis of grain centers and triple points for the YSZ and (Al_2O_3 + B_2O_3) additive samples are given in Table 4. Overall levels of Si indicated may be high due to possible Si contamination during preparation of the TEM samples but the indicated trends were clear. Triple points for both samples were enriched in Al_2O_3, SiO_2 and Y_2O_3 with respect to the grain centers, but were higher in each case for the additive samples. The

amount of Y_2O_3 removed from the grain centers by the boron rich boundary liquid was evdiently not sufficient to cause significant destabilizatin since X-ray diffraction analysis indicated only the cubic zirconia phase being present. Alumina was also enriched on the grain boundaries, as would be expected from the presence of added Al_2O_3 in the flux phase. These observations are in agreement with results obtained by Moghadam et. al.[15] for a similar YSZ powder, except that glass forming impurites such as Ca were not detected by the present analysis.

Table 5 compares 4-point bend strengths for YSZ and YSZ + additive dense samples. Average fracture strengths were slightly lower with Al_2O_3 additions (0.325 wt% Al_2O_3) but maximum strengths were higher than for the YSZ sample. This may result from the larger scatter in the strength data for the Al_2O_3 additive samples due in part to the aforementioned Al_2O_3 particulate inclusions and to the larger average grain size (0.40 μm compared to 0.35 μm for YSZ). For the YSZ samples with added Al_2O_3 and B_2O_3, the strength values obtained were uniformly higher. This may be attributed to the smaller average grain size obtained at the lower temperature and also to differences in composition of the boundary phase. A similar increases in strength values was noted by Kelin on B_2O_3 fluxed Al_2O_3 samples.[24]

Fig. 10 shows thermal expansion ($\Delta\ell/\ell o$) data for the YSZ and additive samples up to ~1000°C. The linearity of the expansion curves and lack of significant hysteresis on heating or cooling illustrated the reheat capability and cubic phase stability throughout the temperature range 25-1000°C.

Fig. 11 shows the optical translucency and infrared transmission spectrum of the (YSZ + 0.65 wt% Al_2O_3 + 0.35 wt% B_2O_3) sample sintered at 1200°C/1.5 hr. Maximum transmission for these samples was approximately 35 percent at ~ 1700 cm^{-1} (~5.9 μ m), the peak IR value for YSZ but transmission was

by longer sintering times or by subsequent hot isostatic pressing of the sintered samples.

Fig. 12 shows dc conductivity data for the YSZ, (YSZ + 0.65 wt% Al_2O_3) and (YSZ + 0.65 wt% Al_2O_3 + 0.3 wt% B_2O_3) samples. Compared to YSZ, conductivity values obtained were higher for the Al_2O_3 and lower for the (Al_2O_3 + B_2O_3) additive samples. The calculated activation energies were 0.97 and 1.01 eV respectively for the Al_2O_3 additive, YSZ and (Al_2O_3 + B_2O_3) additive samples, in line with the conductivity data. For the latter samples, lower a conductivity would be expected from the smaller grain size and higher content grain boundary phase. Similarly, the higher conductivity for the Al_2O_3 additive samples can be attributed to the larger grain size, and simultaneous decrease in the lower conductivity grain boundary area.[15] However, some contribution to the conductivity from the defect substitution of Al^{3+} ions into the Zr^{4+} lattice is considered likely.

CONCLUSIONS

This study has shown that significant enhancement in the densification of high purity, submicron YSZ powders can be achieved by small additions of highly reactive sintering aids such as Al_2O_3 and B_2O_3.

Reductions of up to 150°C in sintering temperature were achieved with 1.0 wt% ($\sim$1.8 vol %) (2:1) Al_2O_3 + B_2O_3 mixture by a demonstrated liquid phase mechanism. Significant temperature reductions were also achieved with 0.3-0.7 wt% Al_2O_3 additions, also attributed to liquid phase assisted sintering.

Mechanical and electrical properties of the sintered YSZ were not degraded by the flux additions, and in some cases were enhanced through closer control of the microstructure and the smaller grain sizes (0.2-0.4 m) achieved.

Analyses carried out by SEM, TEM, X-ray and TMA showed no residual

tetragonal phase, although a small amount in the YSZ might have been expected from the relatively low Y_2O_3 content. Conceivably, any such phase was masked by the cubic YSZ peaks which are very closely positioned.

ACKNOWLEDGEMENTS

This work was supported by the Office of Naval Research under Contract #N-00014-80-K-0969 and in part by the National Science Foundation under MRL grant DMR-80-20250.

TABLE 1

Typical Lot Analysis for

Yttria-Stabilized Zirconia (YSZ) Powders*

Composition (wt%)

Constituent	wt%	Constituent	wt%
ZrO_2	90	SiO_2	0.10
Y_2O_3	7.7	TiO_2	0.06
HfO_2	1.6	Na_2O	0.20
Al_2O_3	0.04	Cl	0.8
CaO	0.30	Cl**	0.04
MgO	0.01		

* Zircar Corp., Florida, NY

** After washing 4 times

TABLE 2

Fired Densities of YSZ and Additives Samples

for Different Sintering Conditions

Sample	Soak Time (h)	Fired Densities 1200°C Bulk (g/cm^3)	1200°C Th.D. (%)	1275°C Bulk (g/cm^3)	1275°C Th.D. (%)	1350°C Bulk (g/cm^3)	1350°C Th.D. (%)
1. [YSZ(8 wt% Y_2O_3)] ($6.022\ g/cm^3$)*	0.5	4.85	80.5	5.30	88.0	5.60	93.1
	4.0	5.37	89.2	5.80	96.3	5.96	99.0
	24.0	5.66	94.0	5.97	99.2	6.003	99.7
2. [YSZ + 0.65 wt% Al_2O_3) ($5.99\ g/cm^3$)*	0.5	5.01	83.7	5.58	96.5	5.97	98.1
	4.0	5.80	96.8	5.91	98.7	5.92	98.9
	24.0	5.92	98.9	5.92	98.9	5.93	99.0
3. [YSZ + 0.65 wt% Al_2O_3 + 0.35 wt% B_2O_3 ($5.95\ g/cm^3$)*	0.5	5.82	98.9	5.89	99.1	5.84	98.1
	4.0	5.89	99.1	5.90	99.2	5.87	98.6
	24.0	5.90	99.2	5.88	98.9	5.85	98.4
4. [YSZ + 0.325 wt% Al_2O_3 ($6.01\ g/cm^3$)*	0.5	5.01	83.5	5.66	94.1	5.91	98.3
	4.0	5.83	97.0	5.92	98.5	5.96	99.2
	24.0	5.95	99.0	5.97	99.3	5.97	99.3
5. [YSZ + 0.325 wt% Al_2O_3 + 0.3 wt% B_2O_3] ($5.96\ g/cm^3$)*	0.5	5.72	96.0	5.80	97.3	—	—
	4.0	—	—	5.90	99.0	5.87	98.6
6. [YSZ + 0.3 wt% Al_2O_3 + 0.7 wt% B_2O_3] ($5.89\ g/cm^3$)*	0.5	5.82	98.8	—	—	—	—
	4.0	5.83	99.0	—	—	—	—

* Calculated Theoretical Densities - (g/cm^3)

Table 2

Incremental Percentage Weight Loss with Temperature

for YSZ and Additive Samples

Soak Temp./Time	Weight Loss		
	YSZ	YSZ + (Al_2O_3 + B_2O_3) (0.65 wt% 0.35) (loss - wt%)	YSZ + (Al_2O_3 + B_2O_3) (1.30 wt% 0.70)
1100°C/1 h	0.0	0.0	0.0
1200°C/1 h	0.08	0.10	0.10
1275°C/1 h	0.03	0.03	0.03
1350°C/1 h	0.06	0.08	0.17
Cum. wt. Loss	0.17	0.21	0.30
Net Loss (B_2O_3)	0.00	0.04	0.13
Amt. B_2O_3 Loss (%)	0.00	11.1	18.5

TABLE 4

EDS Elemental Analysis of Grain Centers and

Triple Points for YSZ and (Al_2O_3 + B_2O_3 Doped Samples

Sample	Elemental Conc. (wt%)				Location
	Al	Si	Y	Zr	
YSZ*	0.24	0.98	7.06	91.70	Grain
YSZ + (Al + B)**	0.31	0.99	6.60	92.1	Center
YSZ*	0.36	3.52	9.14	86.9	Triple
YSZ + (Al + B)**	0.66	3.75	9.90	85.7	Point

* Sintered 1350°C/1.5 h.

** Sintered 1200°C/4 h.; YSZ + (0.65 wt% Al_2O_3 + 0.35 wt% $B2O_3$)

TABLE 4

4-POINT BEND STRENGTHS OF SELECTED

YSZ SAMPLES OF EQUIVALENT DENSITY

Sample	Firing Conditions	Average Strength (MPa)*	Maximum Strength (MPa)
YSZ	1350°C/4h	335±34	338
YSZ + 0.325 wt% Alumina	1350°C/1.5h	310 ± 48	417
YSZ + 0.65 wt% Alumina +	1200°C/1.5h	341 ± 56	453

* 1 STD. Deviation (> 20 samples)

List of Figures

Fig. 8 SEM photomicrographs of polished, thermally etched YSZ samples showing the effects of additive and B_2O_3 loss on the microstructure: a) YSZ-1275°C/4h; b) (YSZ + 0.65 Al_2O_3 + 0.35 B_2O_3 wt%) sample - 1200°C/1.5h; c) (YSZ + 0.325 wt% Al_2O_3) sample - 1275°C/4 h; d) sample b - 1350°C/4h.

Fig. 9 TEM photomicrogrpah of (YSZ + 0.325 wt% Al_2O_3) sample showing liquid phase in grain boundary regions.

Fig. 10 Thermal expansion ($\Delta\ell/\ell o$) data up to 1050°C for YSZ and additive samples.

Fig. 11 IR transmission spectrum and optical translucency of 0.2mm thick YSZ + 0.65 wt% Al_2O_3 + 0.35 B_2O_3) sample fired at 1200°C/4h.

Fig. 12 DC conductivity for YSZ and additive samples as a function of reciprocal temperature for YSZ and additive samples at optimal densities.

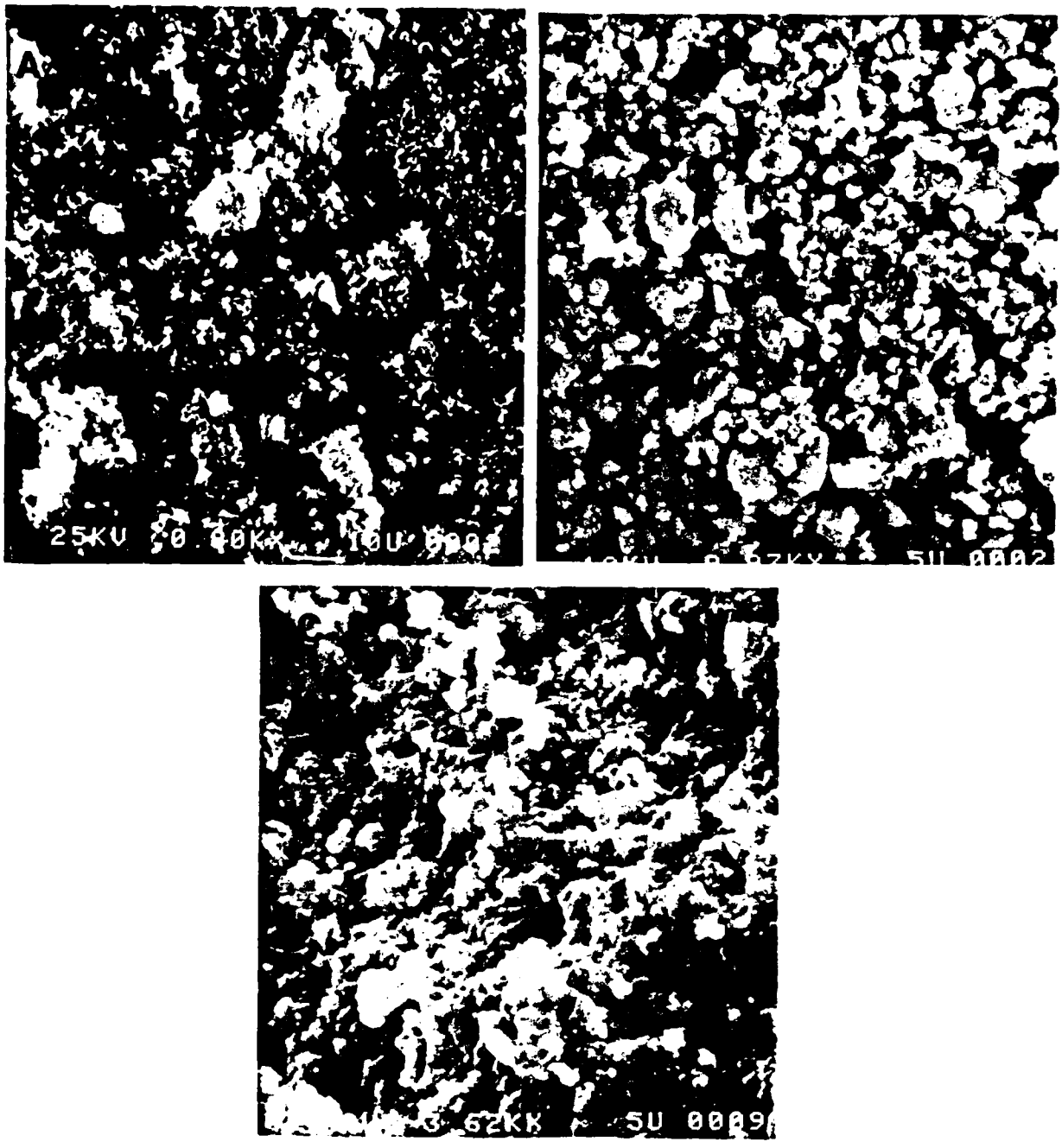

FIG. 1 SEM photomicrographs of submicron YSZ powder showing processing effects: a) as received; b) milled for 12 h; c) milled 12 h, spray dried and pressed 220 MPa.

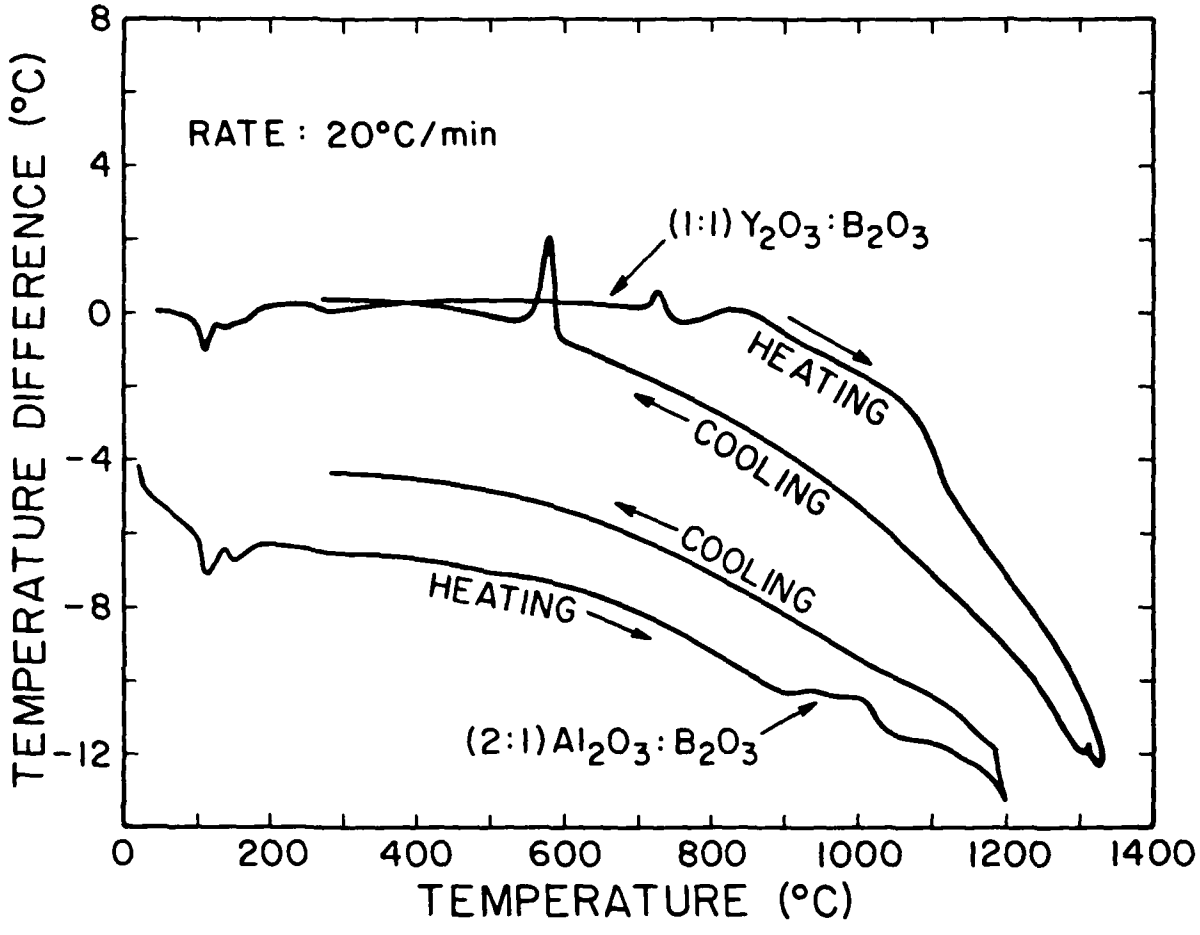

FIG. 2 DTA heating and cooling curves showing reactions of Al_2O_3 and Y_2O_3 with B_2O_3 additive phase.

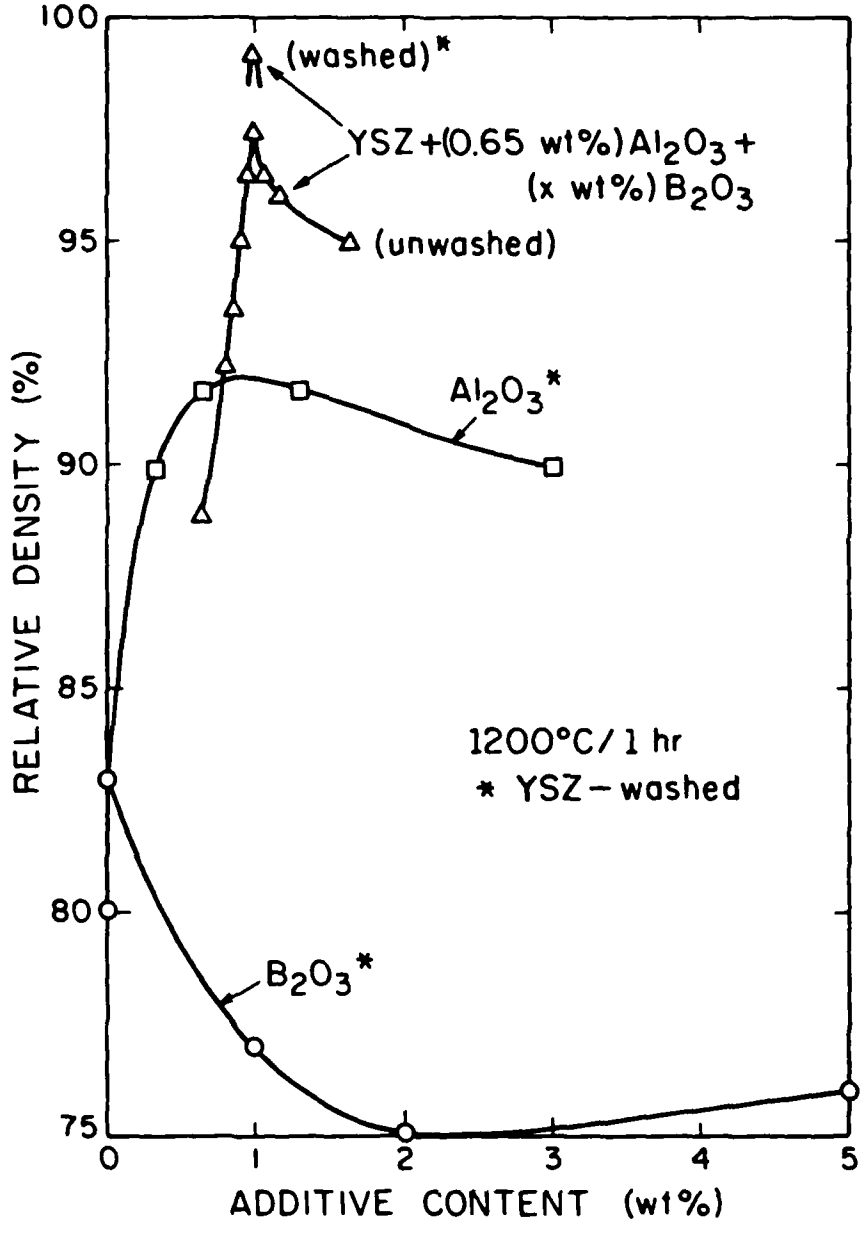

FIG. 3 Additive effects of B_2O_3, Al_2O_3 and (Al_2O_3 + B_2O_3) additives on densification of YSZ. Washed YSZ powders show reduced Cl^- content.

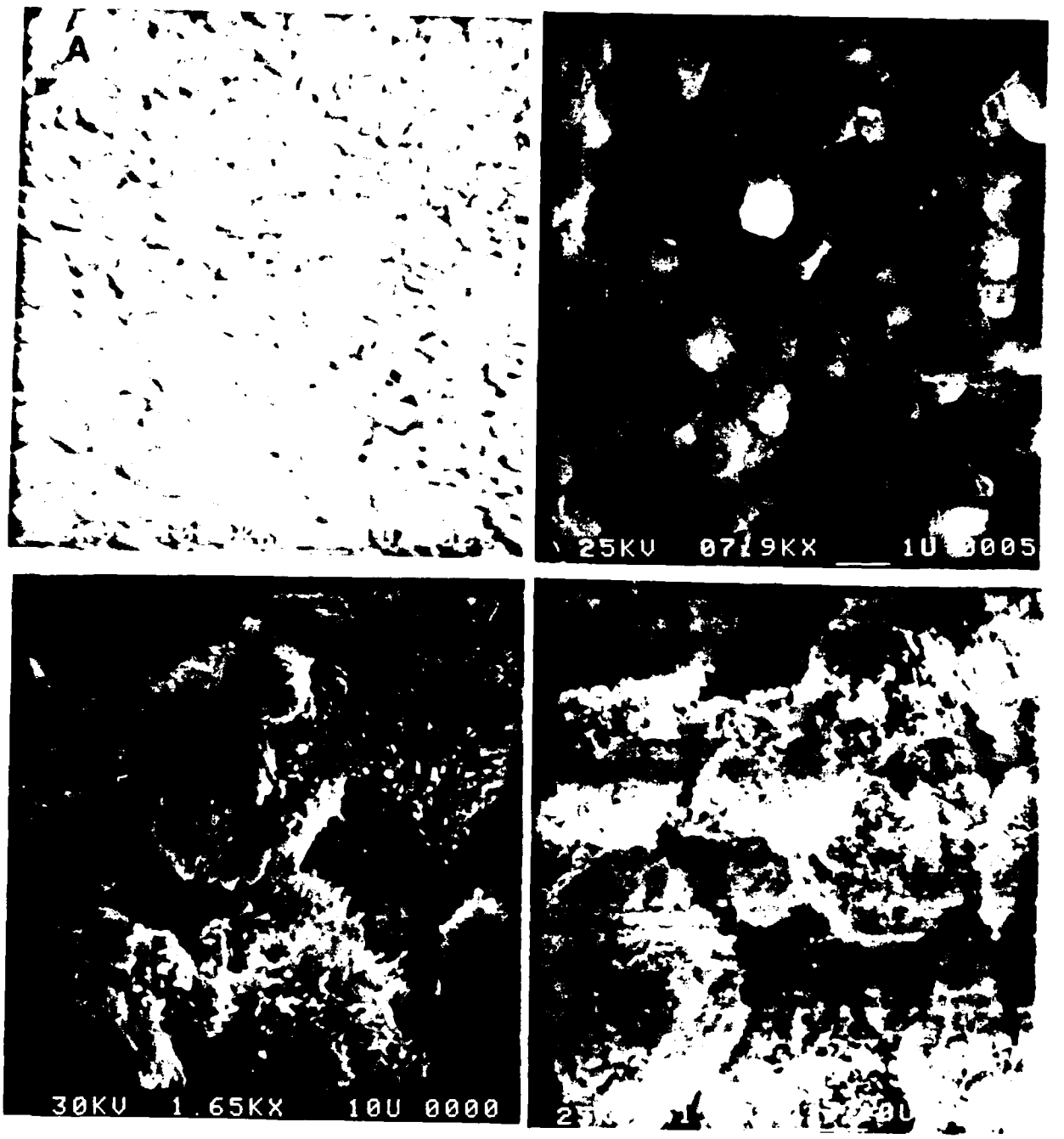

FIG. 4 SEM photomicrographs of additive phases to YSZ reacted at 1200°C/0.5-2 h. a) B_2O_3-0.5 h; b) (1:1) YSZ:B_2O_3-0.5 h. c) (2:1) Al_2O_3:B_2O_3-0.5 h; d) (2:1) YSZ:Al_2O_3-2.0 h.

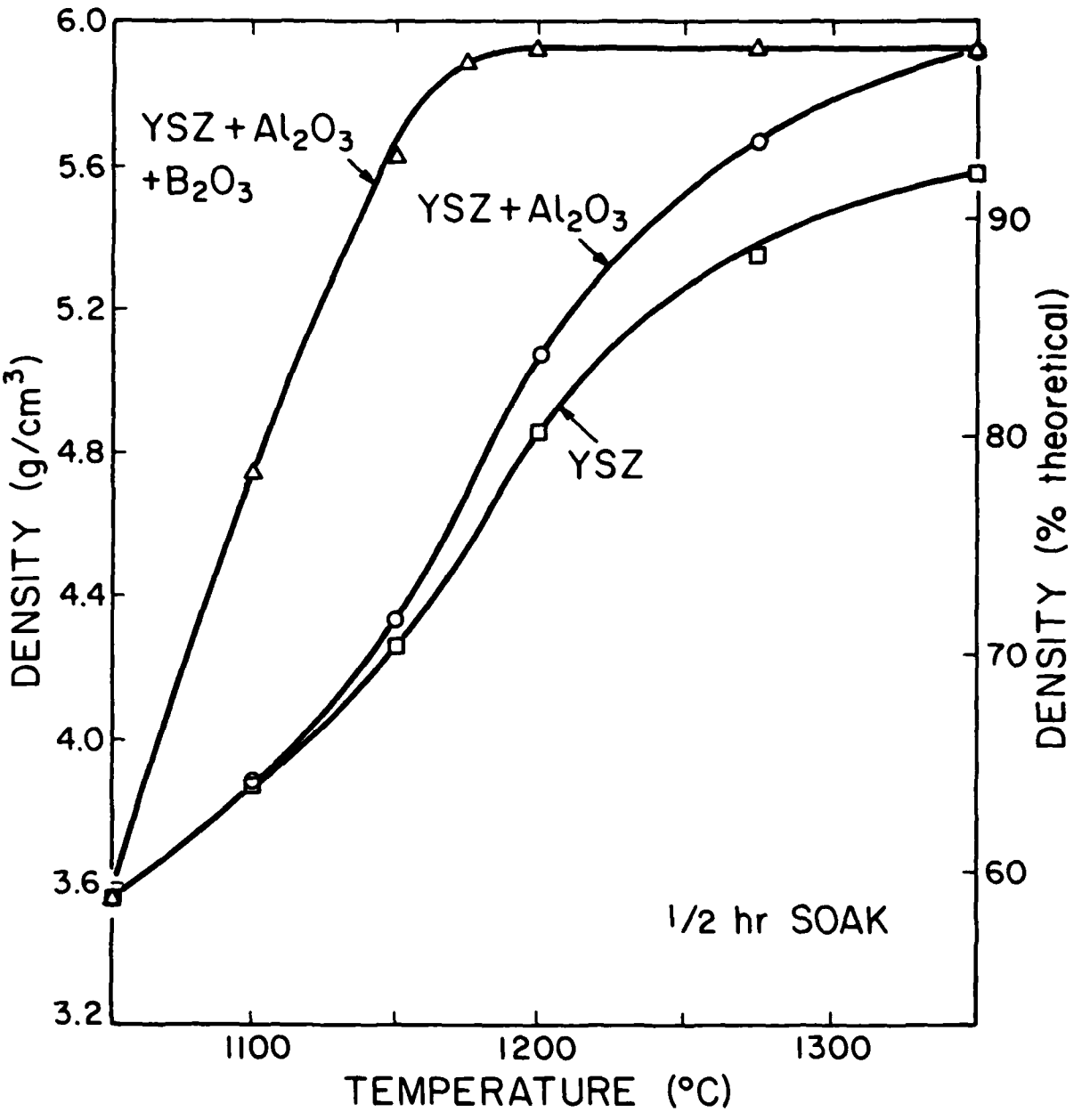

FIG. 5 Densification curves for YSZ samples showing effects of Al_2O_3 and B_2O_3 additives as a function of sintering temperature.

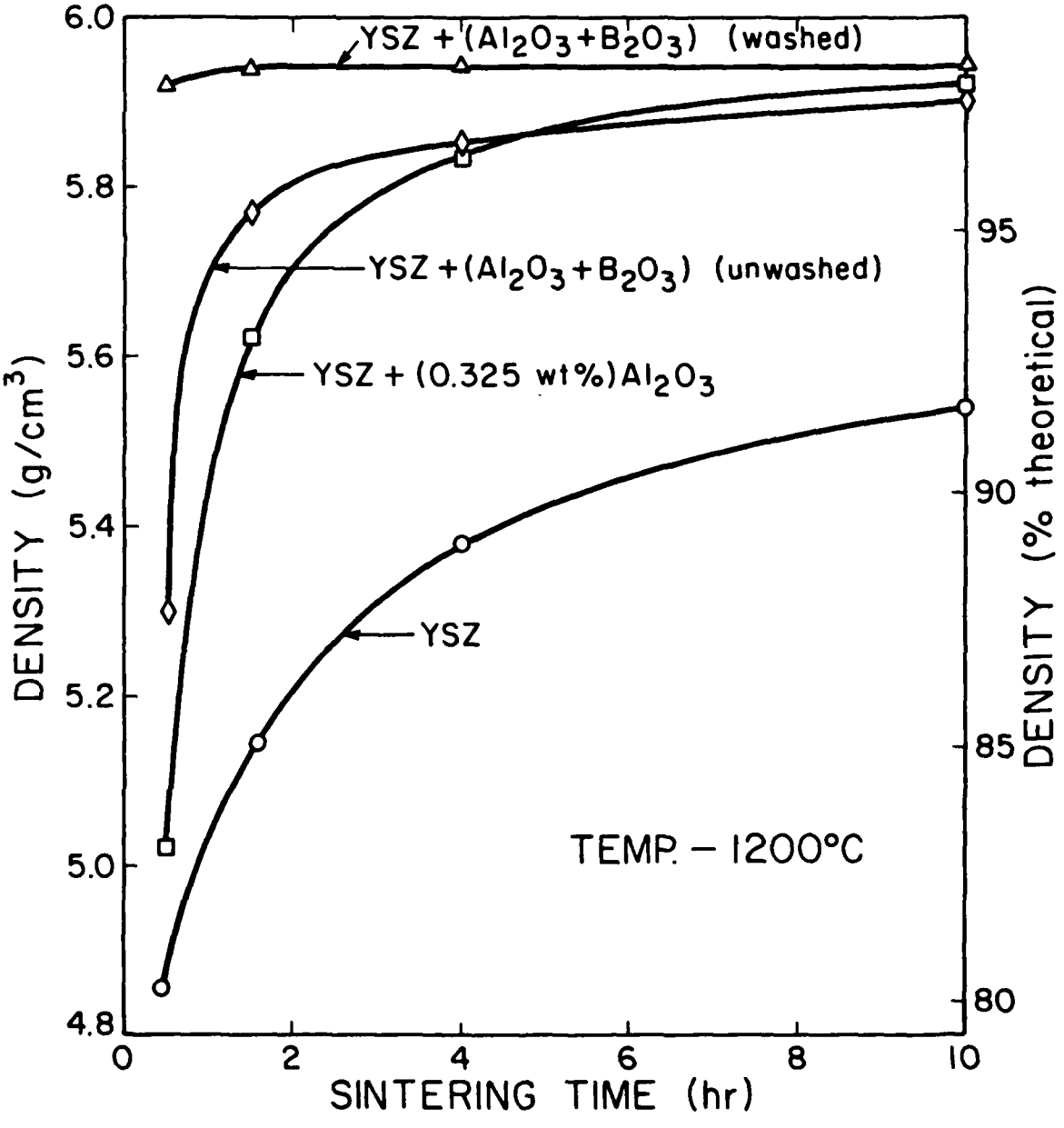

Fig. 6 Densification effects of Al_2O_3 and B_2O_3 additives to YSZ as a function of sintering time.

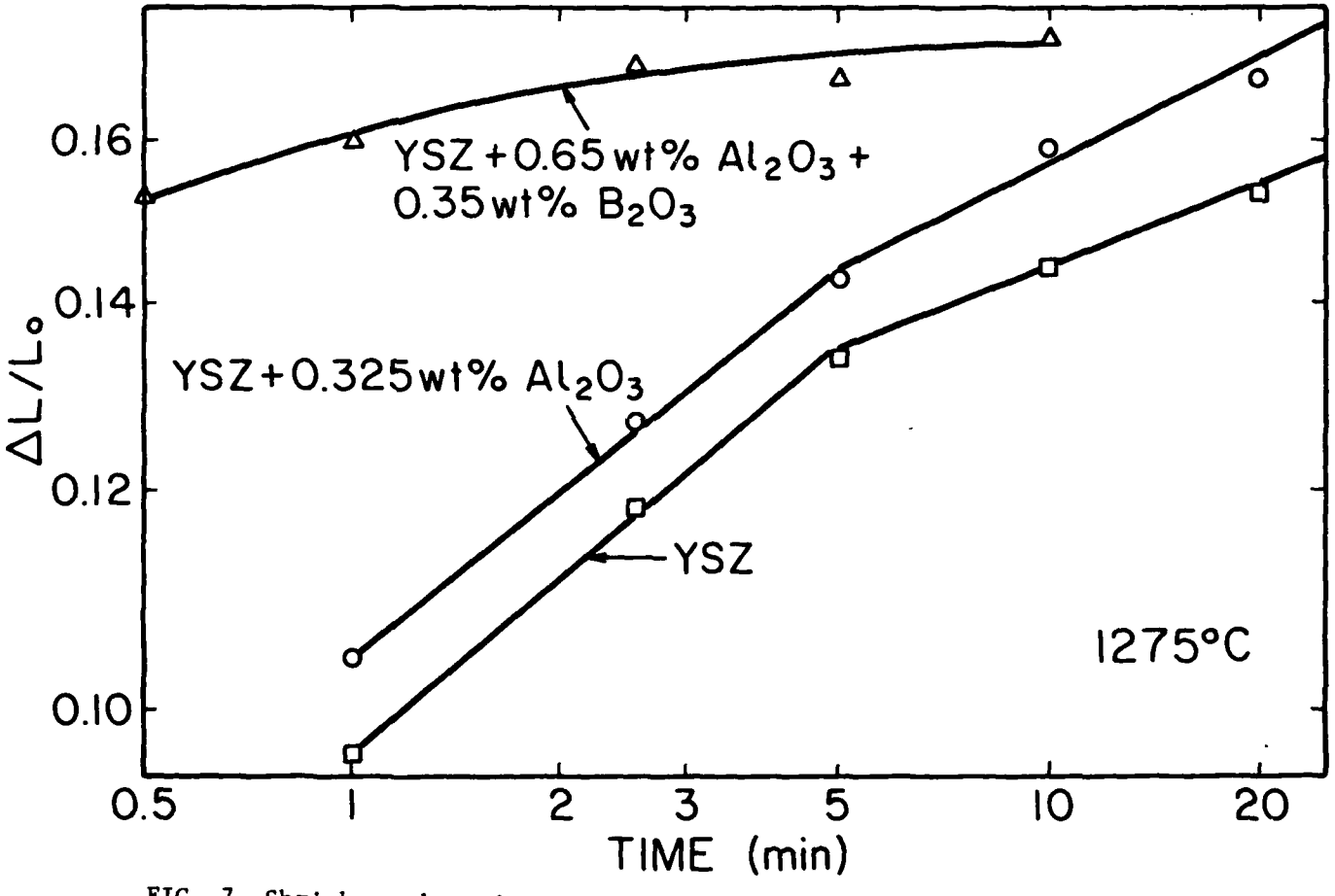

FIG. 7 Shrinkage dependence at 1275°C as a function of time for YSZ and additive samples.

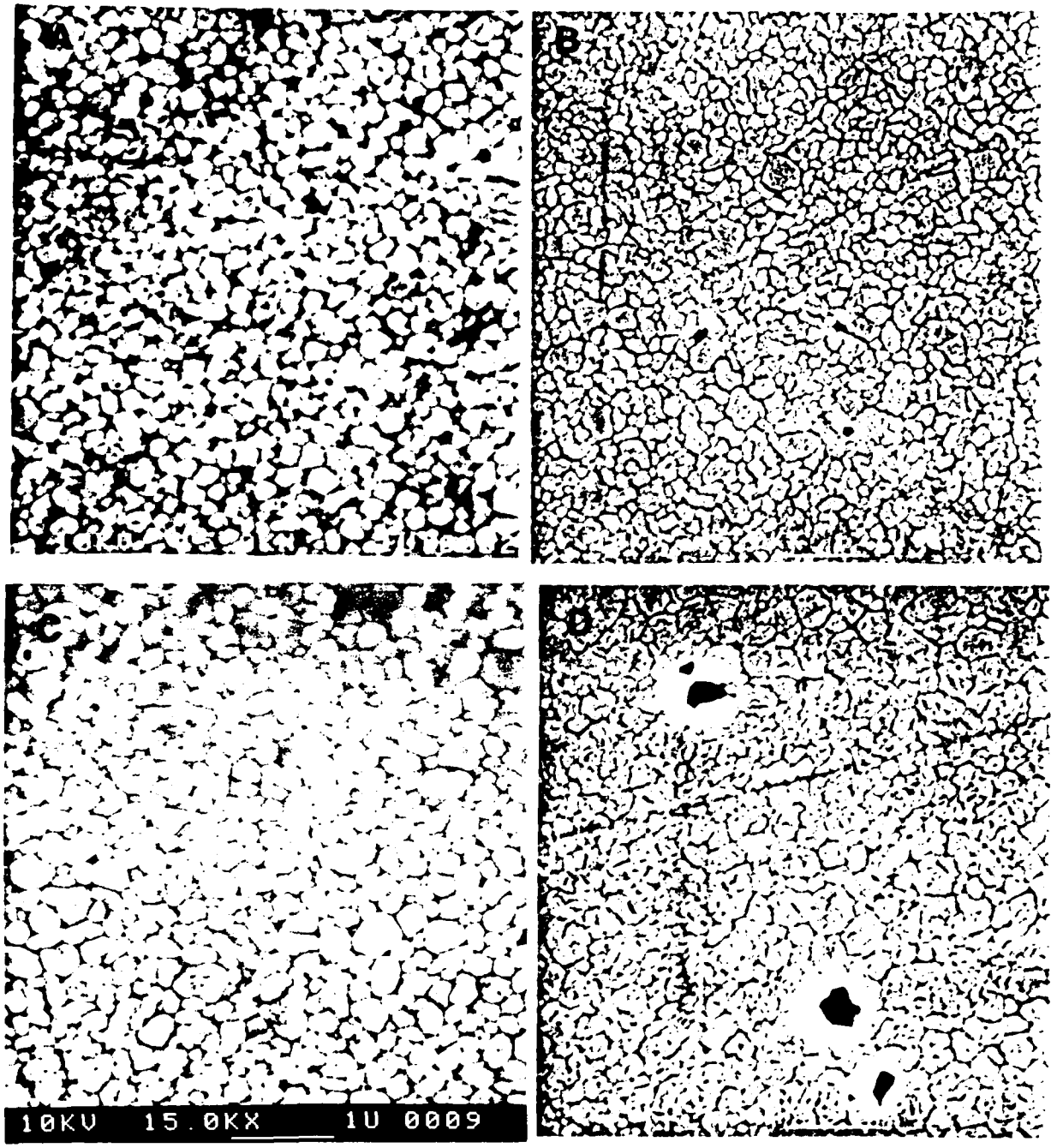

FIG. 8 SEM photomicrographs of polished, thermally etched YSZ samples showing the effects of additive and B_2O_3 loss on the microstructure a) YSZ-1275°C/4h; b) (YSZ + 0.65 Al_2O_3 + 0.35 B_2O_3 wt%) sample - 1200°C/1.5h; c) (YSZ + 0.325 wt% Al_2O_3) sample- 1275°C/4 h; d) sample b - 1350°C/4h.

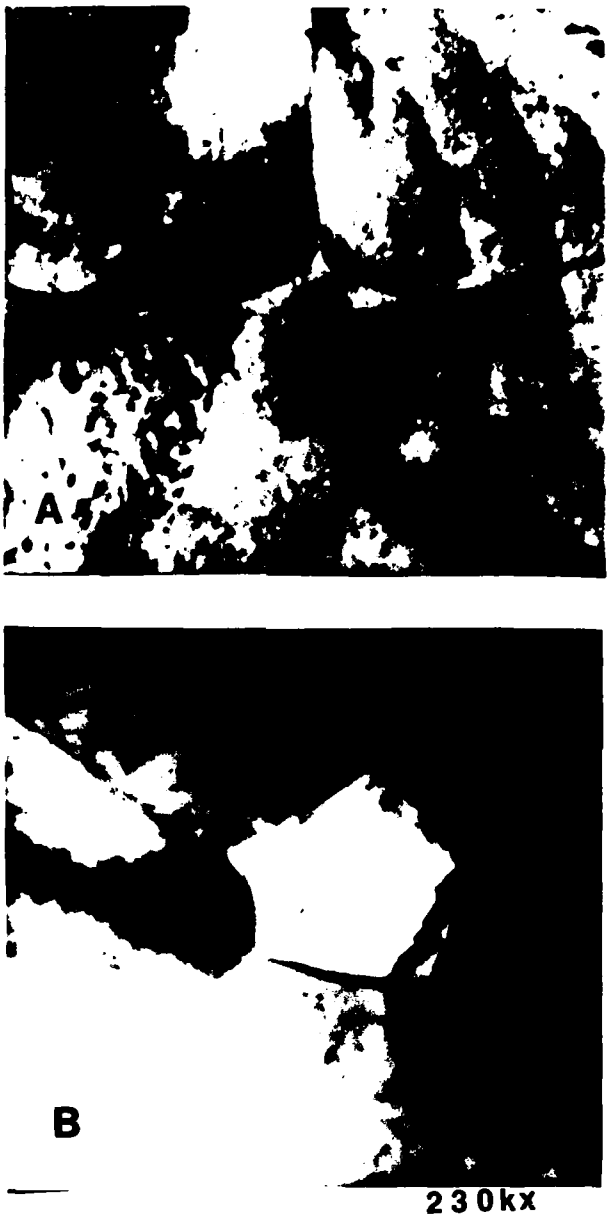

FIG. 9 TEM photomicrograph of (YSZ + 0.325 wt% Al_2O_3) sample showing liquid phase in grain boundary regions.

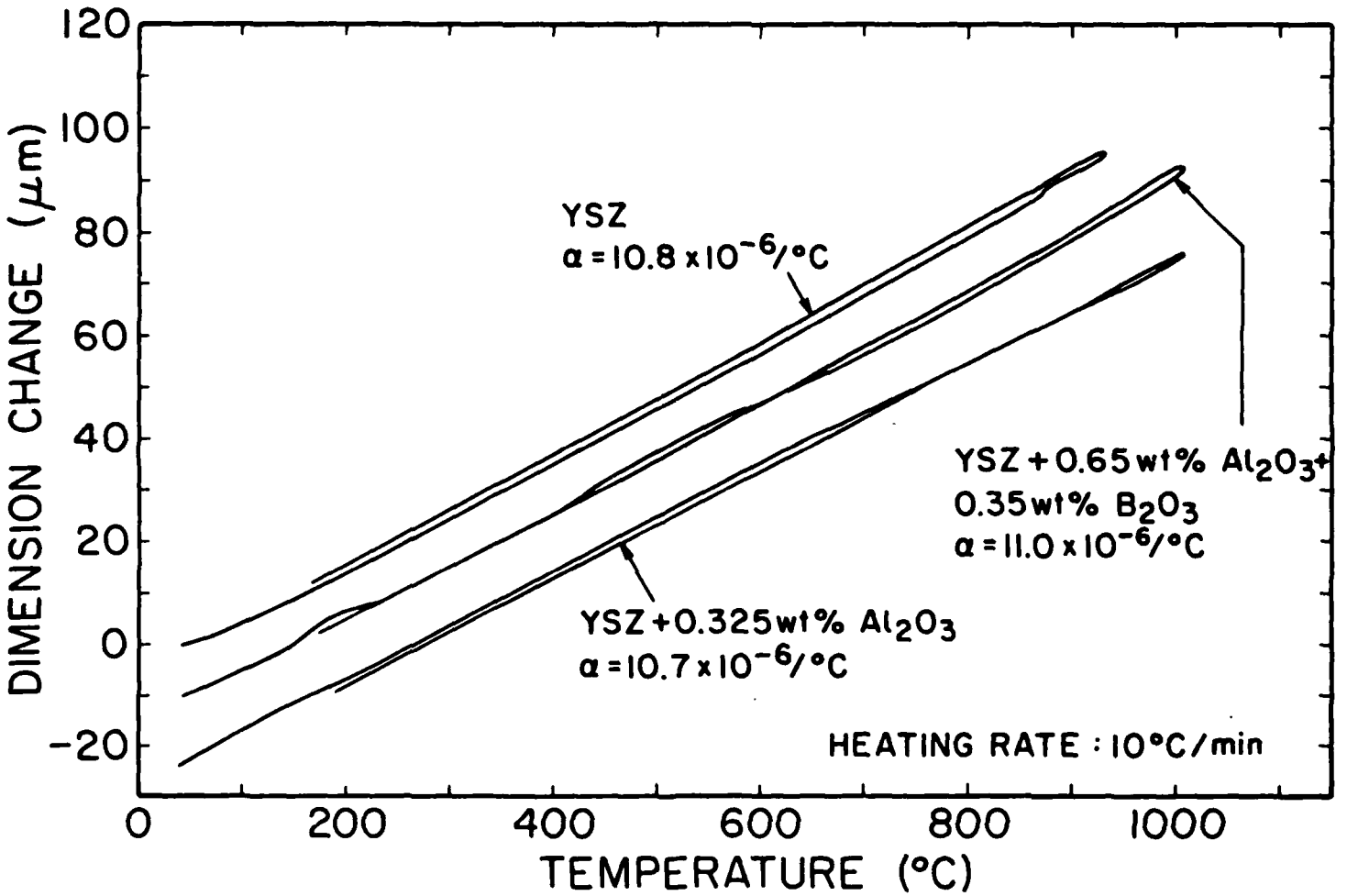

FIG. 10 Thermal expansion ($\Delta\ell/\ell o$) data up to 1050°C for YSZ and additive samples.

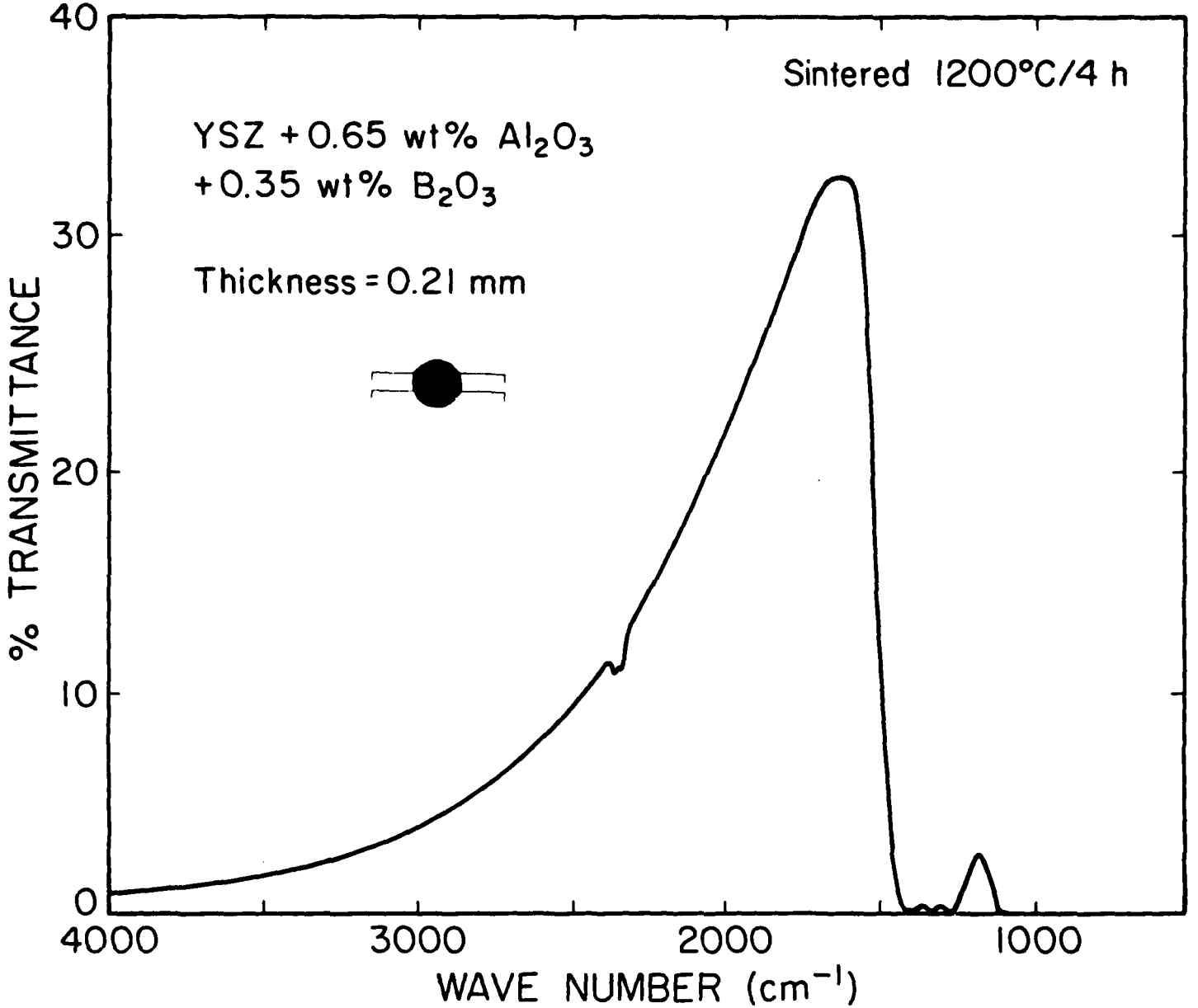

FIG. 11 IR transmission spectrum and optical translucency of 0.2mm thick YSZ + 0.65 wt% Al_2O_3 + 0.35 B_2O_3) sample fired at 1200°C/4h.

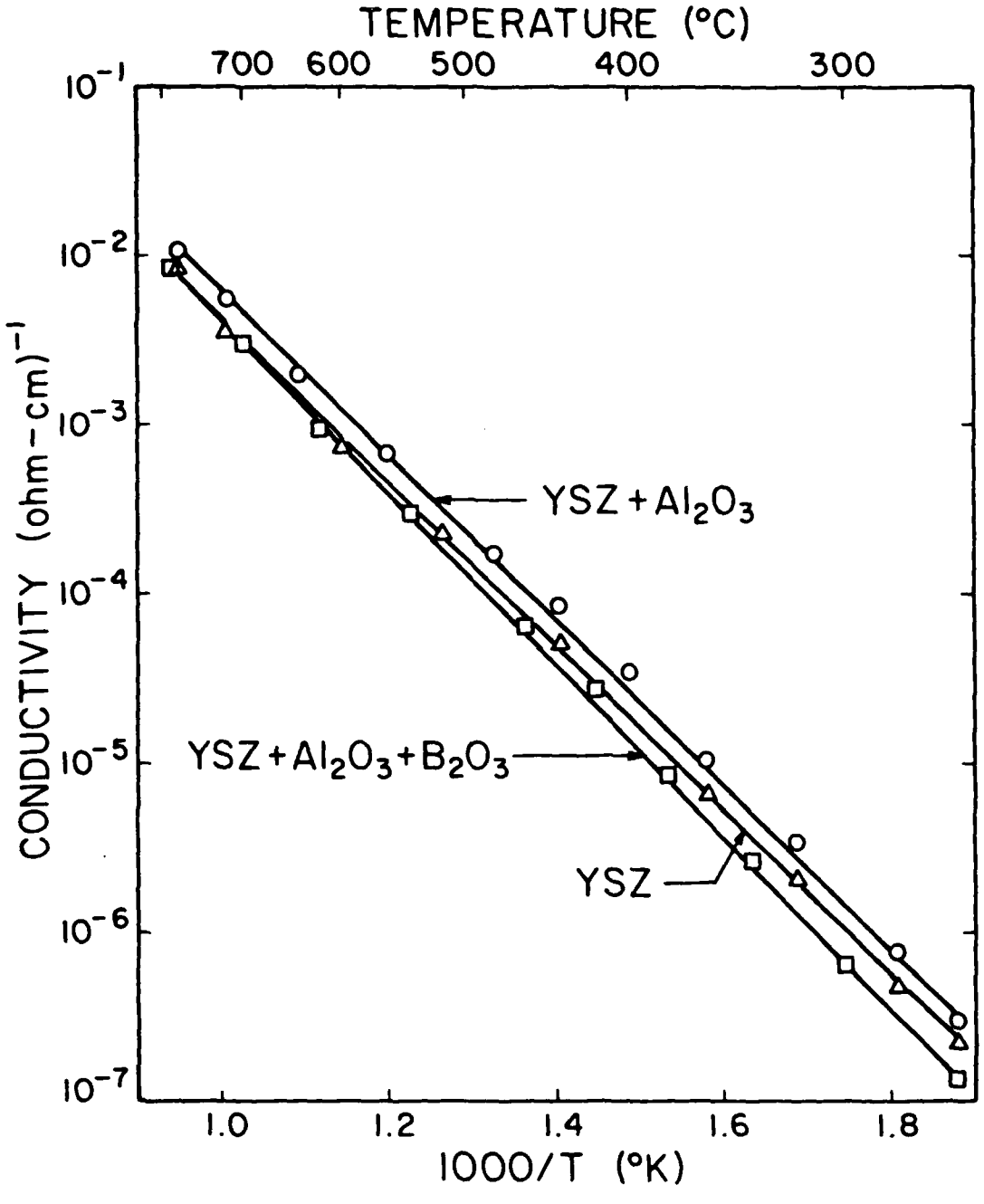

FIG. 12 DC conductivity for YSZ adn additive samples as a function of reciprocal temperature for YSZ and additive samples at optimal densities.

Summary of Work Accomplished
Under Contract No. US NAVY-N-00014-80-K-0969

Reports

Reports issued under this contract include the following:

1. R. C. Buchanan and S. Pope, "Optical and Electrical Properties of Yttria Stabilized Zirconia (YSZ) Crystals," (ONR Report #5), University of Illinois at Urbana-Champaign, Department of Ceramic Engineering, Urbana, IL 61801 (September, 1981).

2. R. C. Buchanan and J. Boy, "Effect of Coprecipitation Parameters on Powder Characteristics and On Densification of PZT Ceramics," (ONR Report #6), University of Illinois at Urbana-Champaign, Department of Ceramic Engineering, Urbana, IL (September 1982).

3. R. C. Buchanan and D. M. Wilson, "Densification of Precipitated Yttria Stabilized Zirconia (YSZ) to Achieve Translucent Properties," (ONR Report #7), University of Illinois at Urbana-Champaign, Department of Ceramic Engineering, Urbana, IL (November 1982).

4. R. C. Buchanan and D. M. Wilson, "Role of Al_2O_3 in Sintering of Submicron Yttria Stabilized ZeO_2 Powders," (ONR Report #8), University of Illinois, Department of Ceramic Engineering, Urbana, IL (December 1983).

5. R. C. Buchanan and D. M. Wilson, "Densification of Submicron YSZ Powders with Alumina and Borate Additives," (ONR Report #9), University of Illinois, Department of Ceramic Engineering, Urbana, IL (December 1984).

6. R. C. Buchanan and J. Boy, "Effect of Powder Characteristics on Microstructure and Properties in Alkoxide Prepared PZT Ceramics," (ONR Report #10), University of Illinois, Department of Ceramic Engineering, Urbana, IL

Thesis

1. G. Wolter, "Properties of Hot-Pressed ZrV_2O_7," M.S. Thesis, University of Illinois, Department of Ceramic Engineering, Urbana, IL, 1981.

2. H. D. DeFord, "Low Temperature Densification of Zirconium Dioxide with Vanadate Additives," M.S. Thesis, University of Illinois, Department of Ceramic Engineering, Urbana, IL, 1982.

3. J. H. Boy, "Effect of Coprecipitation Parameters on the Powder Characteristics of Lead Zirconate Titanate Prepared for Lead Oxide and Butoxide Precursors," M.S. Thesis, University of Illinois, Department of Ceramic Engineering, Urbana, IL, 1983.

4. R. DiChiara, "Processing and Additive Effects on Densification of Calcia Stabilized Zirconia (YSZ)," M.S. Thesis, University of Illinois, Department of Ceramic Engineering, Urbana, IL. 1983.

5. D. M. Wilson, "Effect of Aluminium and Boron oxides on Densification of Yttria Stabilized Zirconia," M.S. Thesis, University of Illinois, Department of Ceramic Engineering, Urbana, IL, 1984.

6. Alena K. Maurice, "Powder Synthesis, Stoichiometry and Processing Effects on Properties of High Purity Barium Titanate," M.S. Thesis, University of Illinois, Department of Ceramic Enginering, Urbana, IL. 1984.

7. S. G. Pope, "Development of Electron Beam Interactive Ceramic Films by RF Sputtering for Memory Applications," M.S. Thesis, University of Illinois, Department of Ceramic Engineering, Urbana, IL, 1984.

Papers

1. D. E. Wittmer and R. C. Buchanan, "Low Temperature Densification of Lead Zirconate Titanate with Vanadium Pentoxide Additive," J. Am. Ceram. Soc., 64 [8] 485-490 (1981).

2. R. C. Buchanan and S. Pope, "Optical and Electrical Properties of Yttria Stabilized Zirconia (YSZ) Crystals," J. Electrochem. Soc., 130, [4] 962-966 (1982).

3. R. C. Buchanan and J. Boy, "Effect of Coprecipitation Parameters on Powder Characteristics and On Densification of PZT Ceramics," Proc. of U.S. Japan Seminar on Dielectrics and Piezoelectrics, Tokyo, Japan, 1982.

4. A. F. Grandin de l'Eprevier and R. C. Buchanan, "Preparation and Properties of $Ca_2V_2O_7$ Single Crystals," J. Electrochem. Soc., 129 [11] 2562-2565 (1982).

5. A. Sircar and R. C. Buchanan, "Densification of CaO-stabilized ZrO_2 with Borate Additives," J. Am. Ceram., 66 [2] 20-21 (1983).

6. G. Wolter and R. C. Buchanan, "Properties of Hot-Pressed ZrV_2O_7," J. Electrochem. Soc., 130 [9] 1905-1910 (1983).

7. R. C. Buchanan, H. D. DeFord, and R. W. Doser, "Effects of Vanadate Phase on Sintering and Properties of Monoclinic ZrO_2," Advances in Ceramics, Vol 7, pp. 196-207, in: Additives and Interfaces in Electronic Ceramics, Am. Ceram. Soc., Columbus, OH (1984).

8. R. C. Buchanan and D. M. Wilson, "Role of Al_2O_3 in Sintering of Yttria Stabilized ZrO_2 Powders," Adv. in Ceramics, Vol. 12, pp. 431-440 [MgO/Al_2O_3 Defect Sintering], Am. Ceram. Society, Columbus, OH (1984).

9. R. C. Buchanan and D. M. Wilson, "Densification of Submicron YSZ Powders with Alumina and Borate Additives," J. Am. Ceram. Soc., 1984 (submitted).

10. R. C. Buchanan and J. Boy, "Effect of Powder Characteristics on Microstructure and Properties in Alkoxide Prepared PZT Ceramics," J. Electrochem. Soc. (1984) (submitted).

Technical Presentations Made (1984)

1. Argonne National Laboratory--"Processing of Submicron Zirconia Powders to Achieve Translucent Properties," 2 h Seminar, (Jan. 1984).

2. Materials Research Conference, "Chemical Synthesis Methods for $BaTiO_3$ and ZrV_2O_7 and Effects on Microstructure and Properties," (Better Ceramics through Chemistry), Albuquerque, N.M. (Feb. 1984). (Poster Presentation).

3. Ferro Corporation, Cleveland, OH, "Review of Chemical Preparation Methods and Processing Parameters for $BaTiO_3$ Powders," Technical Seminar (Feb, 1984).

4. NICE SHORT COURSE, Lecture Presentation on "Synthesis Parameters and Sintering of Ferroelectric Ceramics," (Pittsburgh, PA, April, 1984).

5. American Ceramic Society (Annual Meetings, Pittsburgh, PA, May, 1984). Three technical papers presented: 1) Sol Gel Processing of Thin Dielectric Films from Colloid Precursors; 2) Effect of Al_2O_3 on Strength of Sintered ZrO_2; 3) Processing and Synthesis Effects in High Purity $BaTiO_3$.

6. Ohio State University, Columbus, OH (May, 1984). "Microstructure Development and Grain Boundary Effects in $BaTiO_3$," (Technical Seminar).

7. Center for Professional Advancement, (E. Brunswick, N.J.), Course Director for "Ceramic Applications in Electronics," Five (2-h) Lectures: a) Electronic Ceramics/Dielectrics Properties, b) Glasses and Substrates in Electronics, c) Thick Film Hybrid Circuits; d) Magnetic Ceramics (Ferrites), e) Processing of Electronic Ceramics.

8. GTE Sylvania (Exeter, N.H., September, 1984), 2h Technical Seminar on "Ceramic Sensors, Processing and Future Developments."

9. Pennsylvania State University (State College, PA, Oct., 1984), ONR Technical Review Session, "Processing of Ferroelectric and ZrO_2 Ceramics for Optimal Dielectric and Strength Properties."

10. American Ceramic Society (Pacific Coast Joint Meeting, San Francisco, Nov., 1984). "Processing and Additive Effects on Microstructure and Dielectric Properties of High Purity $BaTiO_3$."

11. US-Japan Seminar on Ferroelectric and Piezoelectric Ceramics (Williamsburg, VA, Nov. 1984), Invited Technical Presentation, "Piezoelectronics, Current Practice and Future Prospects," Poster Presentation, "Grain Boundary Effects on Dielectric Properties of $BaTiO_3$."

END

FILMED

2-85

DTIC